

GEOMETRICALLY MATCHED MULTI-SOURCE MICROSCOPIC IMAGE SYNTHESIS USING BIDIRECTIONAL ADVERSARIAL NETWORKS

Jun Zhuang

Dali Wang

Indiana University-Purdue University Indianapolis
Indianapolis, IN 46202
junz@iu.edu

University of Tennessee
Knoxville, TN 37996
dwang7@utk.edu

ABSTRACT

Microscopic images from different modality can provide more complete experimental information. In practice, biological and physical limitations may prohibit the acquisition of enough microscopic images at a given observation period. Image synthesis is one promising solution. However, most existing data synthesis methods only translate the image from a source domain to a target domain without strong geometric correlations. To address this issue, we propose a novel model to synthesize diversified microscopic images from multi-sources with different geometric features. The application of our model to a 3D live time-lapse embryonic images of *C. elegans* presents favorable results. To the best of our knowledge, it is the first effort to synthesize microscopic images with strong underlie geometric correlations from multi-source domains that of entirely separated spatial features.

Index Terms— Cross domain synthesis, Bidirectional adversarial networks, Multi-source microscopic images, Geometric matching

1. INTRODUCTION

Multi-source observation, which observes the same objective from different sources, has been widely used in many different areas, such as biology and medical fields. For example, microscopic imaging of cell nucleus and membrane separately, with different fluorescent materials, is one kind of multi-source observations. Cross-domain synthesis [2, 7, 6, 3, 5, 1] is one potential solution to augment multi-source observation. Given a source domain A , cross-domain synthesis aims at generating corresponding images of the same objective in a target domain B , or vice versa. According to [2], such synthesis can be divided into two main types, registration-based [7, 6, 3] and intensity-transformation-based methods [5, 1]. The registration-based method assumes that the images within both source and target domain are geometrically related to each other. This method generates images from

a co-registered set of images [7]. On the other hand, the intensity-transformation-based method does not fully rely on the geometric relationship. For example, multimodal is a deep learning approach for MRI image synthesis [1]. The model takes multi-source images as input from source contrasts and yields high-quality images in the target contrast. However, both types of methods mentioned above could not solve the issue that two domains come from different sources with quite different spatial features.

In this study, we propose a new model, **Bidirectional Adversarial Networks for microscopic Image Synthesis (BANIS)**, which uses bidirectional adversarial network to synthesize geometrically matched images from multiple domains. To the best of our knowledge, this model is the first cross-domain synthesis application with multi-source images of entirely separated spatial patterns. We then deploy the model to a set of microscopic images from *C. elegans* embryogenesis to generate diversified, geometrically matched microscopic images. We will make the model source code and the *C. elegans* embryo microscopic dataset publicly available after the paper acceptance.

2. METHODOLOGY

2.1. Preliminary Background

Generative Adversarial Networks (GAN) is one of popular deep learning techniques for cross-domain synthesis. Vanilla GAN [4] consists of two key components, a generator G and a discriminator D . Given a prior distribution Z as input, G maps a point $\mathbf{z} \sim Z$ from the latent space to the data space as $G(\mathbf{z})$. On the other hand, D attempts to distinguish an instance \mathbf{x} from a synthetic instance $G(\mathbf{z})$, generated by G . The training process is set up as if G and D are playing a zero-sum game. On the one hand, G tries to generate the synthetic instances that are as close as possible to real instances. On the other hand, D distinguishes the synthetic instances from the real instances. After the model converges, both G and D reach a Nash equilibrium. At this point, G is able to generate instances which are very close to the real one. The objective function V of Vanilla GAN can be written as a summation of

This study is supported by an NIH research project grants (R01GM097576).

two Expectation values \mathbb{E} as follows:

$$\min_G \max_D V(D, G) = \mathbb{E}_{\mathbf{x} \sim X} [\log D(\mathbf{x})] + \mathbb{E}_{\mathbf{z} \sim Z} [\log(1 - D(G(\mathbf{z})))] \quad (1)$$

where X and Z are the corresponding distribution that \mathbf{x} and \mathbf{z} are sampled from.

In cross-domain synthesis, however, many instances are unpaired between domains [9]. Zhu et al. [9] propose cycle-consistent loss to map the synthetic instances as close as possible to the original instances through the cycled generation, which is combined with two sets of generators and discriminators. The cycle-consistent loss function is described as follows:

$$L_{cyc}(G_A, G_B) = \mathbb{E}_{\mathbf{a} \sim A} [\|G_B(G_A(\mathbf{a})) - \mathbf{a}\|] + \mathbb{E}_{\mathbf{b} \sim B} [\|G_A(G_B(\mathbf{b})) - \mathbf{b}\|] \quad (2)$$

where \mathbf{a} and \mathbf{b} are instances from domain A and B .

2.2. BANIS Model Architecture

The BANIS model (Figure 1) contains two Pioneers P , two Successors S and two Coordinators C . The Pioneer is composed of a Generator G and a Discriminator D . The P is mainly responsible for pre-training in a warm-up stage to speed up the progress of synthesis. The Successor consists of an Encoder E and shares the Generator G with the Pioneer. The S uses its E to compress an input image into latent variables and then uses its G to reconstruct new image from these latent variables. The Coordinator uses pixel-wise methods to preserve the geometric relationship between the images reconstructed by two Successors and the original observed images.

The BANIS model training procedure contains two stages. BANIS simultaneously takes the input images from domain A and domain B . On a warm-up stage, P_A and P_B are trained with given random uniform priors \mathbf{z} and then respectively generate images A_{gen} and B_{gen} . Preliminary images start forming without geometric matching between these images. After the warm-up stage, both S and C join the training to enforce the geometrical relationship between these synthesized images. S_A and S_B learn prior knowledge from observed images, B and A , and reconstruct images with its pre-trained generators from the Pioneers. At the same time, C_A and C_B respectively reinforce the spatial similarity between observed images, B or A , and reconstructed images, B_{rec} and A_{rec} , separately. The model is trained until the geometric relationship between image pairs is formed. After that, we decrease the learning rate of both S and C on subsequent training to improve the quality of synthesized images.

2.3. Loss Functions

The BANIS model uses three types of loss functions to synthesize geometrically matched images. They are Adver-

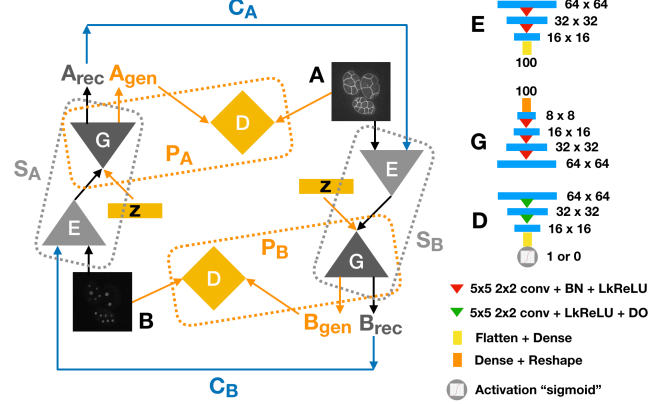


Fig. 1. The model BANIS contains two Pioneers, two Successors, and two Coordinators. The Pioneer is composed of a generator G and a discriminator D . With random uniform priors \mathbf{z} as inputs, P_A and P_B generate images A_{gen} or B_{gen} , respectively. The Successor consists of an encoder E and shares the generator G with the Pioneer. S_A and S_B learn the prior knowledge from observed images, B and A , and reconstruct new images A_{rec} or B_{rec} . By sequentially connect two Successors, the Coordinators C_A and C_B are designed to reinforce the spatial similarity between the reconstructed images, B_{rec} and A_{rec} , and the observed images B and A , separately. The right side of Figure 1 shows an exemplar architecture of E , G and D . The number indicates the size of network layer. For example, encoder E takes 64×64 image as input and outputs a 100-dimension vector of latent variables. 5×5 2×2 conv represents 2D convolutional layer with 5×5 kernel size and 2×2 strides. BN , $LkReLU$ and DO stand for batch normalization layer, LeakyReLU activation layer, and dropout layer, respectively.

arial Loss, Identical Loss and Pair-matched Loss.

Adversarial Loss [4] is employed to enforce the generated image A_{gen} or B_{gen} as similar as possible to the observed image A or B . The adversarial loss is applied to the Pioneer in the whole training process. Given a random uniform prior, however, generated images don't preserve the spatial information between multiple source domains. Note that our model synthesizes the pair of images simultaneously. Thus, this loss is applied to both domain A and domain B .

$$L_{adv}(G, D) = \mathbb{E}_{\mathbf{x} \sim X} [\log D(\mathbf{x})] + \mathbb{E}_{\mathbf{z} \sim Z} [\log(1 - D(G(\mathbf{z})))] \quad (3)$$

Identical Loss is applied to the Successor. To solve previous limitations, the Successor takes specific prior and attempts to reconstruct the images A_{rec} or B_{rec} . Note that the Pioneer helps speed up the synthesis in the warm-up stage. Pioneer's generator is shared with Successor. In other words, reconstructed images are expected to be as close as possible

to both observed images A or B and generated images A_{gen} or B_{gen} . Identical loss ensures the quality of reconstructed images. In this paper, we use mean squared error (MSE) to measure the similarity.

$$L_{id}(S_A, S_B, G_A, G_B) = \mathbb{E}_{\mathbf{b} \sim B, \mathbf{a} \sim A} [\|S_A(\mathbf{b}) - \mathbf{a}\|] + \mathbb{E}_{\mathbf{b} \sim B, \mathbf{z} \sim Z} [\|S_A(\mathbf{b}) - G_A(\mathbf{z})\|] + \mathbb{E}_{\mathbf{a} \sim A, \mathbf{b} \sim B} [\|S_B(\mathbf{a}) - \mathbf{b}\|] + \mathbb{E}_{\mathbf{a} \sim A, \mathbf{z} \sim Z} [\|S_B(\mathbf{a}) - G_B(\mathbf{z})\|] \quad (4)$$

Pair-matched Loss is applied to the Coordinator. This loss enforces the projection inside each Successor to ensure these two domains are spatially matched. The Coordinator sequentially connects these two Successors. C_A takes B as input and uses S_A and S_B sequentially to generate B_{rec} . Then it compares the new images with the observed image B . C_B operates similarly with observed image A . In other words, pair-matched loss helps preserve spatial information among two domains. In this paper, we also use MSE to measure the quality of projection.

$$L_{pm}(C_A, C_B) = \mathbb{E}_{\mathbf{b} \sim B} [\|C_A(\mathbf{b}) - \mathbf{b}\|] + \mathbb{E}_{\mathbf{a} \sim A} [\|C_B(\mathbf{a}) - \mathbf{a}\|] \quad (5)$$

2.4. Geometric Matching Index

Although the individual synthesized images come from different domains and have different geometric patterns, the pair of images that should be geometrically matched. For example, in our microscopic data case, membrane and nucleus should be spatially matched without overlapping. For this purpose, we first extract the binary masks from the reconstructed images from S . Then, we use the Dice Similarity Coefficient (DSC) of two these masks to measure the image overlapping [10]. Less overlapping in our case means better matching. Given an overlapping threshold, such as 0.1 (or 10%, we count the number of well-matched image pairs whose DSC is lower than the threshold, and calculate the percentage of these well-matched image pairs within the total number of image pairs in the newly generated dataset. We defined the percentage as the Geometric Matching Index (GMI) to measure the quality of the BANIS data generation associated with a given threshold.

3. EXPERIMENTS

3.1. Dataset and Preprocessing

We use a set of *C. elegans* microscopy images that contains 15 embryos with ubiquitous fluorescent labeling of cell membrane and nuclei. Each raw image contains one 512×512 membrane image and one 512×512 nuclei image of one to three embryos. Raw images are arranged in sets, each set

contains 100 image stacks taken at 75-second interval over the early stage of embryogenesis. Each stack is a pseudo 3D image that contains 30 slices at 1 μm distance covering the entire embryo(s) [8].

We use ImageJ to split these image stacks and pick the raw images from the middle 15 layers of each stake for our model experiments. We split the raw images into two 512×512 images, each contains membrane- or nuclei-only information. These 512×512 images are then converted to gray scale and denoised with a Gaussian filter. Then, we resized these images into 128×128 for a better computational efficiency. After that, we crop out a single embryo and generate smaller 64×64 images. Finally, we normalize the pixel value of the image between -1 and 1. 10% of images is used as a test set and the rest part is for training. Some samples of the 64×64 microscopic images are illustrated in Figure 2.

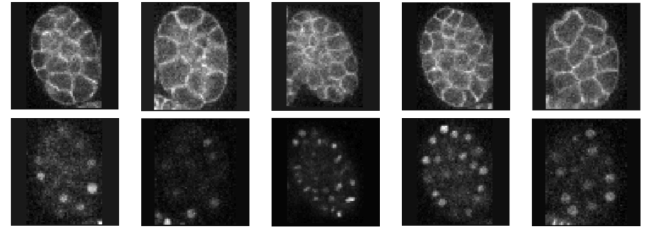


Fig. 2. Samples of the Observed Microscopic Images

3.2. Model Parameters and Training

The shape of input images is $64 \times 64 \times 1$. The latent dimension for both random uniform prior and encoded prior is 100. Both D and P are trained with Adam optimizer. The initial learning rate for G_B is set as 1×10^{-5} and the learning rates for G_A , D_A and D_B are set as 2×10^{-5} . Both S and C are trained with Stochastic Gradient Descent (SGD) optimizer with an initial learning rate of 1×10^{-4} . The batch size is empirically set as 128.

The model is trained with 17,000 epochs in the warm-up stage at the initial learning rate until adversarial the loss converges and the preliminary images start forming. After that, both S and C join the training for subsequent 13,000 epochs until both identical loss and pair-matched loss converge. To improve the quality of synthesized images, both S and C are trained with another 10,000 epochs at a new learning rate, which is decreased by 50%. The total model training with 40,000 epochs takes approximately 12.3 hours on a Linux machine, which configured with 4 Intel Xeon central processing units (E5-1620 v4), 64-GB memory, and a 16-GB Nvidia GP104 graphical processing unit.

After the training, we evaluate the BANIS performance by calculating the GMIs of the entire synthesized dataset with different overlapping thresholds TS_{dsc} . A lower TS_{dsc} indicates a more strictly geometric matched is required.

3.3. Results

After the two-stage training, the BANIS model successfully synthesize satisfactory, geometrically matched image pairs (Figure 3). These synthesized images have clear C.elegans’s image features of membrane or nuclei and simultaneously preserve geometric relationship between them. Note that these images are slices and thus may not display all nuclei in one slice. It is clear that the the generated image pairs have a very similar patterns shown in Figure 2.

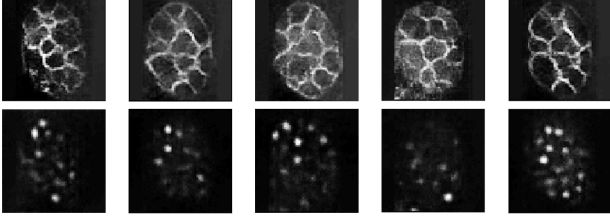


Fig. 3. Exemplar Synthesized Images from BANIS

The result of aforementioned GMI evaluation on the whole synthesized dataset is presented at Table 1. The result reveals that our model yields satisfied synthesized images under strict thresholds TS_{dsc} . Most (over 95%) images of the total image pairs have a overlapping value less than 0.3. Even with a very restrict threshold requirement of 0.1 (that is less than 10% of overlapping between any two simultaneously generated image), the GMI value of the total synthesized image pairs reaches 75.26%.

Table 1. BANIS Data Generation Evaluation

Threshold (TS_{dsc})	0.1	0.2	0.3
GMI (%)	75.26	87.27	95.39

4. CONCLUSION

This study presented a new model, BANIS, to synthesize microscopic images from multiple domains. To the best of our knowledge, BANIS is the first successful model that synthesizes geometrically matched images from multiple domains that have entirely separated spatial patterns. The experiment using microscopic data from C. elegans embryogenesis proved that our model is able to synthesize diversified and geometrically matched images very similar to the observed microscopic images.

5. REFERENCES

- [1] A. Chatsias, T. Joyce, M. V. Giuffrida, and S. A. Tsafaris. Multimodal mr synthesis via modality-invariant latent representation. *IEEE transactions on medical imaging*, 37(3):803–814, 2017.
- [2] S. U. Dar, M. Yurt, L. Karacan, A. Erdem, E. Erdem, and T. Çukur. Image synthesis in multi-contrast mri with conditional generative adversarial networks. *IEEE transactions on medical imaging*, 38(10):2375–2388, 2019.
- [3] G. Erus, J. Doshi, Y. An, D. Verganelakis, S. M. Resnick, and C. Davatzikos. Longitudinally and inter-site consistent multi-atlas based parcellation of brain anatomy using harmonized atlases. *NeuroImage*, 166:71–78, 2018.
- [4] I. Goodfellow, J. Pouget-Abadie, M. Mirza, B. Xu, D. Warde-Farley, S. Ozair, A. Courville, and Y. Bengio. Generative adversarial nets. In *Advances in neural information processing systems*, pages 2672–2680, 2014.
- [5] A. Jog, A. Carass, S. Roy, D. L. Pham, and J. L. Prince. Mr image synthesis by contrast learning on neighborhood ensembles. *Medical image analysis*, 24(1):63–76, 2015.
- [6] J. Lee, A. Carass, A. Jog, C. Zhao, and J. L. Prince. Multi-atlas-based ct synthesis from conventional mri with patch-based refinement for mri-based radiotherapy planning. In *Medical Imaging 2017: Image Processing*, volume 10133, page 10133II. International Society for Optics and Photonics, 2017.
- [7] M. I. Miller, G. E. Christensen, Y. Amit, and U. Grenander. Mathematical textbook of deformable neuroanatomies. *Proceedings of the National Academy of Sciences*, 90(24):11944–11948, 1993.
- [8] D. Wang, Z. Lu, Y. Xu, Z. Wang, A. Santella, and Z. Bao. Cellular structure image classification with small targeted training samples. *IEEE Access*, 7:148967–148974, 2019.
- [9] J.-Y. Zhu, T. Park, P. Isola, and A. A. Efros. Unpaired image-to-image translation using cycle-consistent adversarial networks. In *Proceedings of the IEEE international conference on computer vision*, pages 2223–2232, 2017.
- [10] J. Zhuang, M. Gao, and M. A. Hasan. Lighter u-net for segmenting white matter hyperintensities in mr images. In *Proceedings of the 16th EAI International Conference on Mobile and Ubiquitous Systems: Computing, Networking and Services*, pages 535–539, 2019.